Title
The growth and tensile deformation behavior of the silver solid solution phase with zinc

Authors
Wu, Jiaqi
Lee, Chin C

Publication Date
2016-06-01

DOI
10.1016/j.msea.2016.05.061

Peer reviewed

Materials Science & Engineering A 668 (2016) 160–165

Contents lists available at ScienceDirect

Materials Science & Engineering A

journal homepage: www.elsevier.com/locate/msea

The growth and tensile deformation behavior of the silver solid solution phase with zinc

Jiaqi Wu [a,b,*], Chin C. Lee [a,b]

[a] Department of Electrical Engineering and Computer Science, University of California, Irvine, CA 92697-2660, USA
[b] Materials and Manufacturing Technology, University of California, Irvine, CA 92697-2660, USA

ARTICLE INFO

Article history:
Received 9 April 2016
Received in revised form
15 May 2016
Accepted 16 May 2016
Available online 17 May 2016

Keywords:
Silver-zinc solid solution
Silver
Ingot growth
Electronic packaging
Tensile deformation
Fractography

ABSTRACT

The growth of homogeneous silver solid solution phase with zinc are conducted at two different compositions. X-ray diffraction (XRD) and Scanning electron microscope/Energy dispersive X-ray spectroscopy (SEM/EDX) are carried out for phase identification and chemical composition verification. The mechanical properties of silver solid solution phase with zinc are evaluated by tensile test. The engineering and true stress vs. strain curves are presented and analyzed, with those of pure silver in comparison. According to the experimental results, silver solid solution phase with zinc at both compositions show tempered yield strength, high tensile strength and large uniform strain compared to those of pure silver. Fractography further confirmed the superior ductility of silver solid solution phase with zinc at both compositions. Our preliminary but encouraging results may pave the way for the silver based alloys to be applied in industries such as electronic packaging and structure engineering.

1. Introduction

Silver was firstly mined in about 3000 B.C. in Anatolia (modern day Turkey) [1]. In ancient days, most silver and alloys were used to fabricate coins, bullion and silverware. Nowadays, silver and its alloy still have innumerable applications in arts, science, jewelry, decor, industries, and beyond. According to the report from relevant institute [1], over half of the silver was committed to industrial fabrication in recent five years. The continuing demand of silver in the industry is due to its unique properties such as the best electrical and thermal conductor among metals, high reflectance of light, and the ability to endure high temperature. In history, silver and its alloys have been utilized as filler materials in brazing processes [2,3] in industries, and recently as bonding media in electronics [4,5]. These silver-based joints were reported to be strong, leak-proof, and anti-corrosion. On the other hand, the mechanical properties of silver alloys, such as tensile strength and plasticity, have little been investigated probably because they were not considered as a structural material. With numerous new applications rising on the horizon, the mechanical properties of silver alloys become even more important. For example, in electronic packaging, silver alloys have been proposed as alternative materials for bonding wires [6]. The bonding wires need to have not only good thermal and electrical conductivity but also sufficient tensile strength and elongation [7]. Moreover, the improvement in mechanical properties of silver may not only enhance its performance in traditional applications such as brazing but also exhibit the potential to be utilized in structure engineering. Recently, the Ag-Pd [8] and Ag-Au-Pd [7,9] systems have been reported to have better tensile strength and elongation than pure silver. However, the addition of gold and palladium increases the cost of raw materials. Therefore, it is still a challenge to make silver based alloy both strong and ductile while keeping its low cost.

In spite of these facts, alloying is still a strategy to achieve this goal. Solid solution strengthening mechanism has been well known, responsible for increasing the yield strength of metals as the result of the interactions between the solutes and dislocations. According to the Ag-Zn phase diagram [10], which is shown in Fig. 1, the solid solubility of zinc in silver is about thirty atomic percent (30 at%) at 100 °C. This value will be smaller at room temperature but zinc concentration as large as 25 at% was acquired in the literature [11]. The solid solubility is quite substantial which makes Ag-Zn system appear as a promising candidate. In addition, recall that alpha brass, the copper solid solution phase with zinc, is stronger than pure copper and still very ductile and thus suitable for cold working and many other structure attempts [12] Moreover, silver and copper are in the same column in the periodic table and thus have similar valence electron configuration. This gives rise to an interesting question: whether alloying zinc into silver can make the alloy both strong and ductile?

Usually, the total dopant concentration in silver alloys is below

* Corresponding author at: Department of Electrical Engineering and Computer Science, University of California, Irvine, CA 92697-2660, USA.
E-mail address: jiaqw10@uci.edu (J. Wu).

http://dx.doi.org/10.1016/j.msea.2016.05.061
0921-5093/

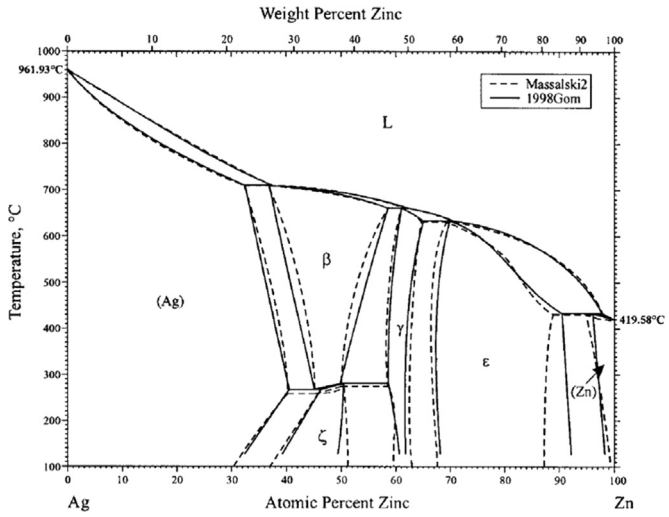

Fig. 1. Silver-zinc binary phase diagram.

15 at%, such as sterling silver (Ag-12.1 at%Cu), Ag-Pd [8] and Ag-Au-Pd system [7,9]. As a preliminary study of Ag-Zn system, we chose to grow and characterize silver solid solution phases with 5 at% and 15 at% zinc concentration, respectively, which are designated as (Ag)-5Zn (3.1 wt%) and (Ag)-15Zn (9.6 wt%). Meanwhile, pure silver was used as the controlled group for the following experiments [13].

In the following section, the preparation method of the ingots of (Ag)-5Zn and (Ag)-15Zn and test samples will be firstly presented. Secondly, the process and results of materials characterization will be described. Next, the engineering and true stress vs. strain curve which are acquired in tensile test will be discussed. In addition, the fracture surface of the tensile specimen will be examined by Scanning Electron Microscope (SEM) and the fracture mode and failure mechanism will be analyzed. Lastly, the potential application and scientific value of the research will be discussed.

2. Experimental procedures

2.1. Preparation of ingots

In our research, the ingots of (Ag)-5Zn and (Ag)-15Zn were prepared by melting raw materials under vacuum. The starting materials were 99.99% silver shots and 5N zinc shots. Next, the shots were uniformly mixed and loaded into a quartz tube with 15 cm in length and 1 cm in inner diameter. While the quartz tube was being pumped by vacuum pump, it was sealed by hydrogen torch at the position which is between the pump end and metallic shots. The vacuum within the capsule can effectively mitigate the oxidation issue and reduce defects such as gas trapped bubble in the final products. Then the capsule was placed into a furnace preheated at 1030 Celsius and kept isothermal for 3 h for adequate homogenization. Lastly, a six-stage cooling profile between 1030 Celsius and room temperature was designed for acquiring homogenous solid solution phase. More specifically, the temperature of each dwell stage was determined by the homologous temperature (Th) which expresses the temperature of material as a fraction of its melting temperature using Kelvin. The materials were cooled down from 0.95 to 0.3 (lower than 100 Celsius) in 8 days and the cooling between adjacent stages were quite fast and done within 2 h.

Disk samples, cut from the ingots by slow speed saw, were ground and polished carefully for material characterization. X-Ray Diffraction (XRD) and Energy Dispersive Spectroscopy (EDX) were

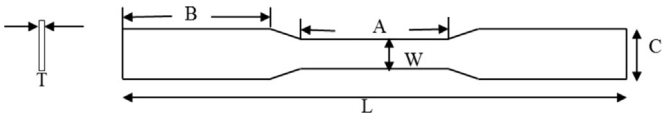

Fig. 2. The geometry of tensile specimen, in accordance with ASTM E8/E8M-08.

Table 1.
The dimensions of tensile specimen, in accordance with ASTM E8/E8M-08.

	W	T	L	A	B	C
mm	2	1.1	33.33	10.67	10	3.33
inch	0.0787	0.0433	1.3120	0.4200	0.3937	0.1311

carried out to verify if the solid solution phase with nominal composition was successfully prepared. Rigaku SmartLab diffractometer was used for phase identification. Tests were conducted by using Bragg-Brentano (BB) optics since the samples are bulk polycrystalline materials. The θ-θ scan was operated at 2° per minute with a filter removing copper k-beta line. FEI XL-30 FEG SEM equipped with EDX system was used for chemical composition analysis. Test areas were randomly chosen from the samples and data was collected from nine points per area in which the average spacing between adjacent points is 75 μm.

The tensile specimens from each ingots were machined by electrical discharge machining (EDM) in accordance with ASTM E8/E8M-08 specification [14]. In Fig. 2 and Table 1, the geometry and dimension are shown respectively. These samples were carefully polished in order to remove surface damage caused by EDM and then annealed at 200 Celsius for 1 h to release residue stress induced by polishing. After annealing process, XRD and EDX were conducted and results were compared to those of disk samples. The uniaxial tensile tests were performed at room temperature by INSTRON 5500R tester with a nominal strain rate of about $10^{-5}\ s^{-1}$. After fracture, the specimens were observed by SEM to reveal deformation morphologies and fracture behavior.

3. Results and discussion

3.1. XRD and EDX results

XRD results of pure silver, (Ag)-5Zn and (Ag)-15Zn disk samples are shown in Fig. 3. The data collected in the tests were processed and analyzed by PDXL, an integrated powder XRD analysis software package. The peaks in Fig. 3 are indexed and the crystallography information of samples are acquired and listed in Table 2.

From Fig. 3, it is apparent that the crystal structure of pure silver, (Ag)-5Zn and (Ag)-15Zn are face centered cubic (FCC) in terms of diffraction patterns' systematic absence. In addition, there are no impurity peaks other than the peaks of pure silver, (Ag)-5Zn and (Ag)-15Zn in each XRD pattern. Therefore, it is conservatively concluded that the materials composing the disk samples are nearly homogeneous. In Table 2, d is d-spacing between corresponding crystallographic plane, (hkl) is the Miller's indices with classic denotation, and a is the calculated lattice constant by using values of each d-spacing under the assumption that the geometry of lattice is perfect cubic. As results, the weighted average value for lattice constants are 4.0893 Å, 4.0796 Å and 4.0623 Å for pure silver, (Ag)-5Zn and (Ag)-15Zn respectively. The trend of decreasing values for lattice constant is consistence with the right-shifted peaks in XRD patterns, which can be explained by reviewing the atomic radii for silver and zinc elements. The empirical atomic radii of zinc is 134 pm, which is smaller than that of silver's, 144 pm. Therefore, if one silver atom is replaced by zinc in silver lattice, it would result in dent in its crystal structure, which caused

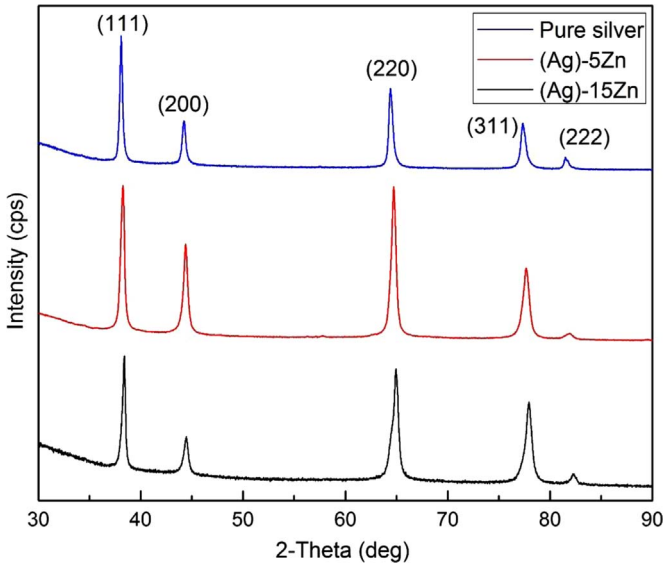

Fig. 3. XRD pattern of Pure silver (blue), (Ag)-5Zn (red) and (Ag)-15Zn (black). (For interpretation of the references to color in this figure legend, the reader is referred to the web version of this article.)

Table 2.
(a) Peak list and analysis results of pure silver.

Peak #	2-Theta (deg)	d (Å)	(hkl)	a (Å)
1	38.092	2.3605	(111)	4.0885
2	44.221	2.0455	(200)	4.0910
3	64.382	1.4459	(220)	4.0896
4	77.328	1.2330	(311)	4.0894
5	81.493	1.1801	(222)	4.0880

(b) Peak list and analysis results of (Ag)-5Zn

Peak #	2-Theta (deg)	d (Å)	(hkl)	a (Å)
1	38.204	2.3539	(111)	4.0771
2	44.277	2.0441	(200)	4.0882
3	64.618	1.4412	(220)	4.0763
4	77.546	1.2300	(311)	4.0794
5	81.770	1.1769	(222)	4.0769

(c) Peak list and analysis results of (Ag)-15Zn

Peak #	2-Theta (deg)	d (Å)	(hkl)	a (Å)
1	38.404	2.3421	(111)	4.0566
2	44.441	2.0369	(200)	4.0738
3	64.925	1.4351	(220)	4.0591
4	77.843	1.2261	(311)	4.0665
5	82.300	1.1707	(222)	4.0554

the decrease in lattice constant as the concentration of zinc increased. Besides, the lattice distortion makes the crystal not a perfect cubic any more, which induces the slight difference between calculated lattice constants in Tables 2(b) and (c) by using different D-spacing from the same solid solution phase.

EDX results of (Ag)-5Zn and (Ag)-15Zn disk samples are listed in Table 3. For both compositions, the measured zinc concentration are nominal concentration with small deviation. In consideration of the limitation of EDX and our group's facility condition, the errors are acceptable and the nominal composition can be regarded as real composition.

Table 3.
EDX (point and shoot mode) results for (Ag)-5Zn and (Ag)-15Zn.

	(Ag)-5Zn		(Ag)-15Zn	
	Ag (at%)	**Zn (at%)**	**Ag (at%)**	**Zn (at%)**
Average concentration	94.49%	5.51%	85.01%	14.99%
Standard deviation	0.53%		1.25%	

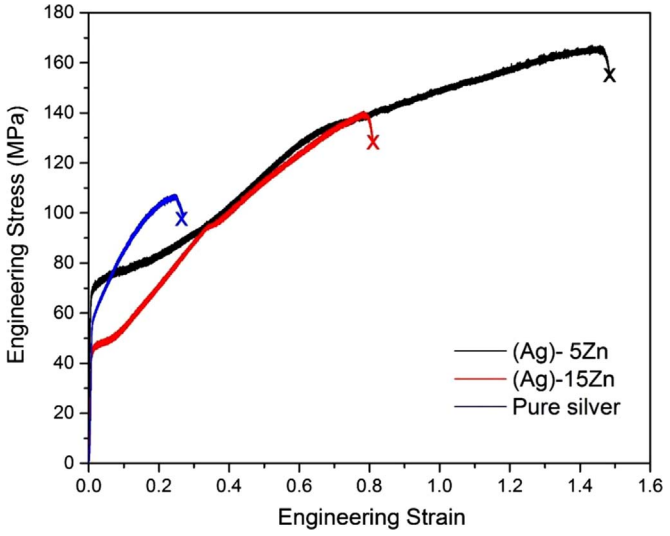

Fig. 4. Engineering stress vs. strain curve of pure silver (blue), (Ag)-5Zn (black) and (Ag)-15Zn (red). (For interpretation of the references to color in this figure legend, the reader is referred to the web version of this article.)

The XRD and EDX results shown above are representative and repeatable for disk samples' crystallography and chemical composition examination. Besides, the results of tensile samples which are from different region of the ingots show the consistency. In conclusion, nearly homogeneous polycrystalline (Ag)-5Zn and (Ag)-15Zn have been successfully prepared by melting raw materials under vacuum and cooling down following specific annealing profiles. Even so, further efforts and improvement can be made to improve the quality of the ingots.

3.2. Tensile test

In consideration of the limitation of our facility and preparation process, defects such as cavities of which the size is in micron range exist in the ingots. Besides, tensile test samples are cut from different regions of the ingots. Therefore, the quality and orientation distribution of grains of these samples may vary a little from one to another. In our current research, multiple rounds of tests are conducted on each specific composition. Representative results of pure silver, (Ag)-5Zn and (Ag)-15Zn will be discussed. Fig. 4 exhibits the engineering stress vs. strain curve of pure silver, (Ag)-5Zn and (Ag)-15Zn. To get a true indication of the deformation characteristics of materials, true stress vs. true strain curve (known as flow curve) are also plotted and shown in Fig. 5. The calculation of true stress and true strain are based on (Eqs. (1) and 2), in which s is engineering stress, e is engineering strain, σ is true stress and ε is true strain.

$$\sigma = s(e+1) \tag{1}$$

$$\varepsilon = \ln(e+1) \tag{2}$$

According to the flow curve, all three materials start with linear elastic deformation and then transit into plastic stage. The transition behavior of silver solid solution phase is quite different from that of pure silver's. For Pure silver, the transition is relatively smooth and followed strain hardening rate is high. However, sharp transition occurs in solid solution phase and followed with a low strain hardening region. This phenomenon can be interpreted as the interaction between dislocation and Short-Range Order (SRO) in the solid solution phase [15]. Although the solute arrangement in solid solution phase is disordered in long range in our cases, SRO

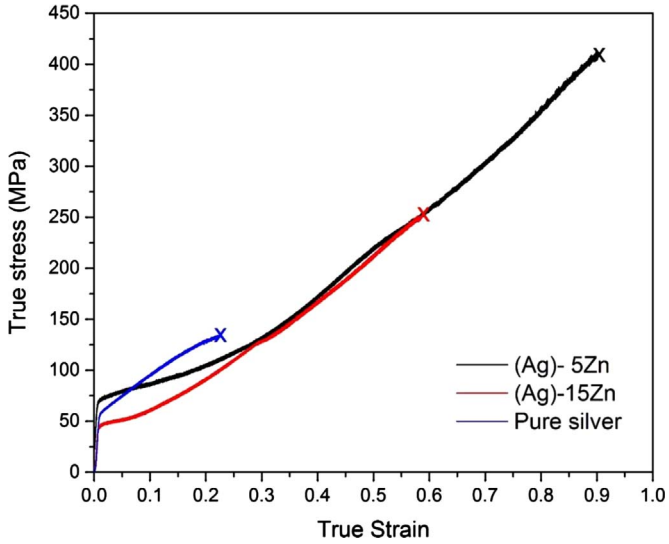

Fig. 5. True stress vs. strain curve of pure silver (blue), (Ag)-5Zn (black) and (Ag)-15Zn (red). (For interpretation of the references to color in this figure legend, the reader is referred to the web version of this article.)

may occur with the increase of the solute concentration. The SRO can be an obstacle for the dislocation to glide in the lattice. When the leading dislocation begins to glide, the SRO is destroyed. Since the order is only of a short range, it won't be restored and the following dislocations can glide easily on this plane [16]. This phenomenon is also referred as glide plane softening. As a result, a yield point effect [17] or low strain hardening rate at low strains [18] is found in solid solution phase with FCC structure.

The yield strength, ultimate tensile strength, uniform strain, true stress at maximum load and true uniform strain are summarized and listed in table. Here, true stress at maximum load is used instead of true fracture stress because true fracture stress should be corrected for the triaxial state of stress existing in the tensile specimen at fracture. However, the data required for this correction are often not available, true fracture values are thus frequently in error. Similarly, true uniform strain is used since it's impossible to calculate true fracture strain simply through fracture elongation for tensile specimen with rectangular cross section.

According to Table 4, the yield strength of (Ag)-5Zn is higher than that of pure silver while (Ag)-15Zn shows a decrease in yield strength. Based on classical solid solution strengthening theory for coarse-grained polycrystalline such as those from Fleischer [19] and Labusch [20], the solid solution will be further strengthened with the increase in solute concentration. Therefore, the decrease in yield strength of (Ag)-15Zn seems abnormal in consideration of the traditional theory. However, this phenomenon can be referred as solid solution softening, which is not limited to metallic system but has also been reported in covalent and ionic systems [21]. It is possible, therefore, that a common but unknown mechanism may exist for this phenomenon. In literatures, solid solution softening in body-centered cubic (BCC) crystal structure has been most extensively studied in the past. In iron-carbon system, a mechanism has been developed by examining the motion of a screw dislocation through a combination of Peierls field and misfit strain centers [22]. In Molybdenum based solid solution, the softening additions will locally alter the chemical bonding which results in a decrease of the generalized stacking fault energy and atomic row shear resistance [23]. It is also reported that the addition of zinc will soften the secondary glide systems in magnesium based solid solution phase of which the crystal structure is hexagonal-closed packed (HCP) [24]. For silver solid solution phase with indium (FCC), solid solution strengthening occurs in dilute indium concentration [25] while a decrease in yield strength has been reported when the atomic concentration of zinc is higher than 9.5% [13]. From well-studied systems, the interaction between dislocation and localized structure that induced by solute contribute to the decrease in yield strength. In our case, in view of the localized factors that can influence the mobility of dislocation, the ease of destroying SRO for the leading dislocation in (Ag)-15Zn may partially contribute to the softening phenomenon. However, further quantitative research and modelling are needed to evaluate solid solution softening and the critical solute concentration between softening and hardening for solid solution phase with FCC structure.

Table 4.
Summary of tensile test results with pure silver as comparison.

Composition	Yield strength (MPa)	Ultimate tensile strength (MPa)	Uniform strain (%)	True stress at maximum load (MPa)	True uniform strain (%)
Pure silver	56.6	106.7	25	133.8	22
(Ag)-5Zn	68.5	166.5	148	412.2	92
(Ag)-15Zn	48.2	127.4	90	250.0	65

It is also noticeable that the uniform strain of (Ag)-5Zn is 148% which is about 5 times larger than that of pure silver. For (Ag)-15Zn, the uniform strain is 90% which is smaller than that of (Ag)-5Zn but still shows substantial increase compared to pure silver. Even in limited report on pure silver [26], the uniform strain is smaller than 50% under room temperature. Moreover, from Table 4, the true stress at maximum load of (Ag)-5Zn is more than 3 times that of pure silver. Similarly, (Ag)-15Zn shows the decrease in strength compared to (Ag)-5Zn but is still superior to pure silver. Recall that any point on the flow curve can be considered as the yield strength for a metal strained in tension by the amount shown on the curve. Thus, if the load is removed at this point and then reapplied, the material will behave elastically throughout the entire range of reloading. Therefore, the huge increase in true stress at maximum load is highly remarkable since it indicates that the yield strength of silver solid solution phase can be largely increased by cold work such as forging and rolling. In total, (Ag)-5Zn and (Ag)-15Zn not only increase the true stress at maximum load but also exhibit much better ductility compared to pure silver. The materials will hopefully show better mechanical properties if the quality is further improved.

3.3. *Fractography*

The fracture surface of (Ag)-5Zn and (Ag)-15Zn are examined by using SEM to analyze the failure mode. The images at different magnification for (Ag)-5Zn and (Ag)-15Zn are shown in Figs. 6 and 7, respectively.

According to Fig. 6(a), the necking of (Ag)-5Zn tensile samples is rather serious so that the parts above and below the neck separate along an extremely narrow plane of which the width is less than 100 μm. Compared to the original thickness of the tensile sample, 1.1 mm, the width of cross section is reduced by a factor of 12. In addition, the surface is featureless and smooth. For (Ag)-15Zn, as shown in Figs. 7(a) and (b), the topography of fracture surface is similar as that of (Ag)-5Zn. The only difference is that the final width of the fracture plane is a little bit larger, which is an indication that the ductility is decreased compared to that of (Ag)-5Zn. However, the shrinkage in cross section of (Ag)-15Zn is still remarkable.

This type of fracture mode is called rupture, which is induced by localization of plastic deformation. More specifically, in tensile test, for specimen with rectangular cross section, there are two

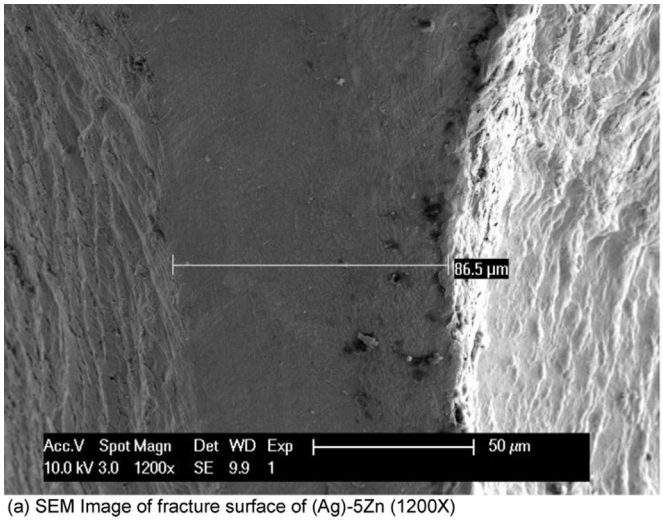

(a) SEM Image of fracture surface of (Ag)-5Zn (1200X)

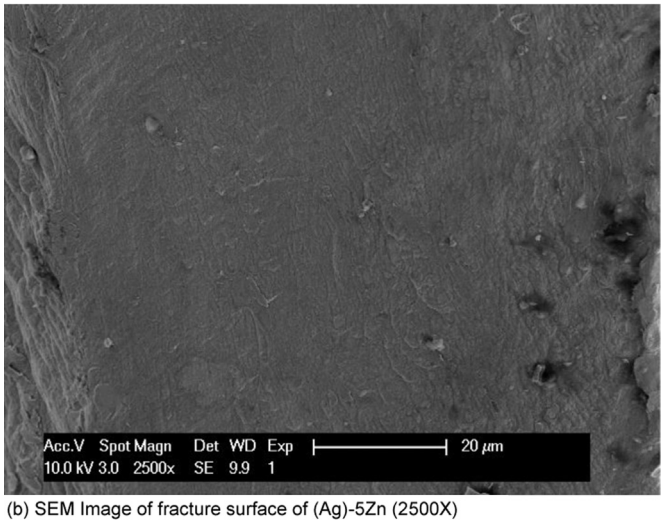

(b) SEM Image of fracture surface of (Ag)-5Zn (2500X)

Fig. 6. (a) SEM Image of fracture surface of (Ag)-5Zn (1200 ×). (b) SEM Image of fracture surface of (Ag)-5Zn (2500 ×).

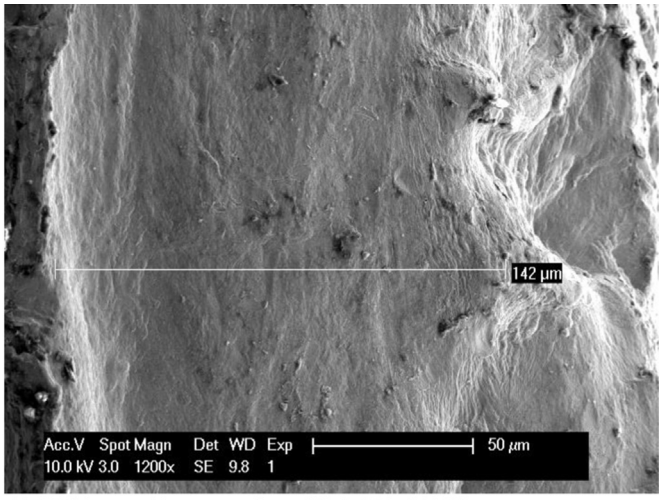

(a) SEM Image of fracture surface of (Ag)-15Zn (1200X)

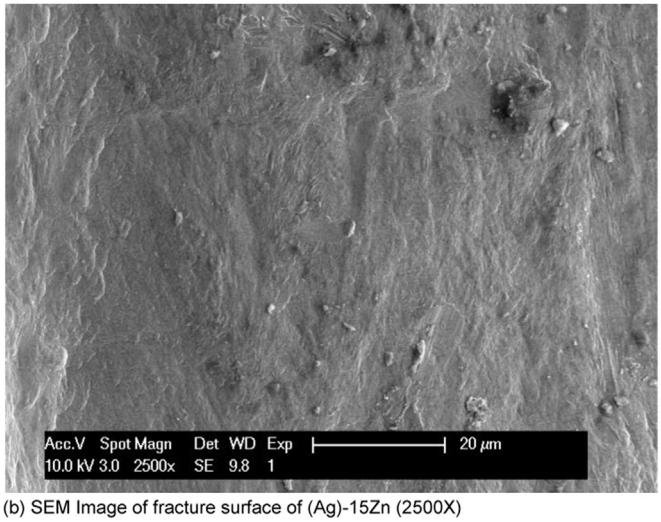

(b) SEM Image of fracture surface of (Ag)-15Zn (2500X)

Fig. 7. (a) SEM Image of fracture surface of (Ag)-15Zn (1200 ×). (b) SEM Image of fracture surface of (Ag)-15Zn (2500 ×).

types of tensile flow instability. The first is diffuse necking, which induces the shrinkage in width. Diffuse necking may terminate in fracture but usually it's not serious and followed by second instability process called localized necking [27]. In this mode, continued thinning around one section finally leads to fracture. Orowan [28] proposed that rupture is a strong indication that the material is very ductile. In conclusion, the results of fractography show the consistency with the tensile test data, confirming that the ductility of silver solid solution phase with zinc is enhanced compared to that of pure silver.

4. Conclusions

In this paper, the ingots of silver solid solution phase with zinc have been successfully prepared at two compositions. A preliminary evaluation of mechanical property has been conducted by tensile test. Solid solution strengthening phenomenon is observed in (Ag)-5Zn while solid solution softening occurs in (Ag)-15Zn. The tensile test results also indicate that the addition of certain amount of zinc into silver will not only largely increase the ductility but also the strength. Therefore, the silver solid solution phase with zinc is a promising candidate for bonding wire and interconnect medium in microelectronics industry. Future efforts will be made to investigate the other properties of silver solid solution with zinc such as electrical conductivity and reflectivity.

Acknowledgment

XRD and SEM/EDX work were performed at the UC Irvine Materials Research Institute (IMRI).

References

[1] The Silver Institute, World Silver Supply and Demand, (accessed 18.01.16), ⟨https://www.silverinstitute.org/site/supply-demand/⟩, 2016.
[2] A. Rabinkin, F. Reidinger, J. Marti, L. Bendersky, Processing, structure and performance of RS "classical" silver-base brazing alloys, Mater. Sci. Eng.: A 133 (1991) 256–260.
[3] A. Elrefaey, W. Tillmann, Interface characteristics and mechanical properties of the vacuum-brazed joint of titanium-steel having a silver-based brazing alloy, Metall. Mater. Trans. A 38 (12) (2007) 2956–2962.
[4] R.W. Chuang, C.C. Lee, Silver-indium joints produced at low temperature for high temperature devices, IEEE Trans. Compon. Packag. Technol. 25 (3) (2002) 453–458.
[5] C.-X. Yang, X. Li, G.-Q. Lu, Y.-H. Mei, Enhanced pressureless bonding by tin doped silver paste at low sintering temperature, Mater. Sci. Eng.: A 660 (2016) 71–76.
[6] C. Lu, Review on silver wire bonding, Int. Micro Pack. Ass., 2013, pp. 226–229.
[7] T.-H. Chuang, C.-H. Tsai, H.-C. Wang, C.-C. Chang, C.-H. Chuang, J.-D. Lee, et al., Effects of annealing twins on the grain growth and mechanical properties of Ag-8Au-3Pd bonding wires, J. Electron. Mater. 41 (11) (2012) 3215–3222.

[8] T.-H. Chuang, H.-J. Lin, C.-H. Chuang, Y.-Y. Shiue, F.-S. Shieu, Y.-L. Huang, et al., Thermal stability of grain structure and material properties in an annealing twinned Ag–4Pd alloy wire, J. Alloy. Compd. 615 (2014) 891–898.
[9] L.J. Kai, L.Y. Hung, L.W. Wu, M.Y. Chiang, D.S. Jiang, C. Huang, et al., editors, Silver alloy wire bonding, in: IEEE 62nd Electronic Components and Technology Conference (ECTC), 2012.
[10] H. Okamoto, Ag-Zn (Silver-Zinc), J. Phase Equilib. 23 (5) (2002) 454.
[11] W.B. Pearson, A Handbook of Lattice Spacings and Structures of Metals and Alloys: International Series of Monographs on Metal Physics and Physical Metallurgy, Elsevier, 2013.
[12] V. Raghavan, Physical metallurgy: Principles and Practice, PHI Learning Pvt. Ltd, New Delhi, India, 2015.
[13] Y.J. Huo, C.C. Lee, The growth and stress vs. strain characterization of the silver solid solution phase with indium, J. Alloy. Compd. 661 (2016) 372–379.
[14] ASTM standard E8/E8M-08, Standard test methods for tension testing of metallic materials, ASTM International, West Conshohocken, PA, 2008, ⟨http://dx.doi.org/10.1520/E0008_E0008M-08⟩, www.astm.org.
[15] J.C. Fisher, On the strength of solid solution alloys, Acta Metall. 2 (1) (1954) 9–10.
[16] V. Gerold, H.P. Karnthaler, On the origin of planar slip in f.c.c. alloys, Acta Metall. 37 (8) (1989) 2177–2183.
[17] T. Steffens, C. Schwink, A. Korner, H.P. Karnthaler, Transmission electron microscopy study of the stacking-fault energy and dislocation structure in CuMn alloys, Philos. Mag. A 56 (2) (1987) 161–173.
[18] N. Clement, D. Caillard, J.L. Martin, Heterogeneous deformation of concentrated Ni-Cr F.C.C. alloys: macroscopic and microscopic behavior, Acta Metall. 32 (6) (1984) 961–975.
[19] R.L. Fleischer, Substitutional solution hardening, Acta Metall. 11 (3) (1963) 203–209.
[20] R. Labusch, A Statistical theory of solid solution hardening, Phys. Status Solidi B 41 (2) (1970) 659–669.
[21] A. Sato, M. Meshii, Solid solution softening and solid solution hardening, Acta Metall. 21 (6) (1973) 753–768.
[22] D. Quesnel, A. Sato, M. Meshii, Solution softening and hardening in the iron-carbon system, Mater. Sci. Eng. 18 (2) (1975) 199–208.
[23] N.I. Medvedeva, Y.N. Gornostyrev, A.J. Freeman, Solid solution softening in bcc Mo alloys: effect of transition-metal additions on dislocation structure and mobility, Phys. Rev. B 72 (13) (2005) 134107.
[24] A.H. Blake, C.H. Cáceres, Solid-solution hardening and softening in Mg-Zn alloys, Mater. Sci. Eng.: A 483–484 (2008) 161–163.
[25] H. Suga, T. Imura, Solid-solution hardening of silver single-crystals by indium, by tin and by antimony, Jpn. J. Appl. Phys. 14 (8) (1975) 1253–1254.
[26] J.E. Bailey, P.B. Hirsch, The dislocation distribution, flow stress, and stored energy in cold-worked polycrystalline silver, Philos. Mag. 5 (53) (1960) 485–497.
[27] G.E. Dieter, Mechanical Metallurgy, third ed., Mc Graw Hill, NY, 1986.
[28] E. Orowan, Fracture and strength of solids, Rep. Prog. Phys. 12 (1) (1949) 185.